Control Optimisation of CO_2 Cycles for Medium Temperature Retail Food Refrigeration Systems

Y.T. Ge*, S.A. Tassou

Mechanical Engineering, School of Engineering and Design, Brunel University, Uxbridge, Middlesex, UB8 3PH, UK

ABSTRACT

This paper describes a detailed procedure into the investigation of optimised control strategies for CO_2 cycles in medium temperature retail food refrigeration systems. To achieve this objective, an integrated model was developed composing of a detailed condenser/gas cooler model, a simplified compressor model, an isenthalpic expansion process and constant evaporating temperature and superheating. The CO_2 system can operate subcritically or transcritically depending on the ambient temperature. For a transcritical operation, a prediction can be made for optimised refrigerant discharge pressures from thermodynamic cycle calculations. When the system operates in the subcritical cycle, a floating discharge pressure control strategy is employed and the effect of different transitional ambient temperatures separating subcritical and transcritical cycles on system performance is investigated. The control strategy assumes variable compressor speed and adjustable air flow for the gas cooler/condenser to be

modulated to achieve the constant cooling load requirement at different ambient conditions.

Keywords: CO_2, Thermodynamic cycle, Refrigeration, Modelling, Control, Optimisation

* Corresponding author. Tel.:+44 1895 266722; fax: +44 1895 256392.
E-mail address:yunting.ge@brunel.ac.uk

Nomenclature

A	area (m^2)	*Subscripts*	
C_p	specific heat at constant pressure ($J\ kg^{-1}K^{-1}$)	a	air
C	capacity rate ($W\ K^{-1}$)	amb	ambient
d	diameter(m)	dis	discharge
D	depth (m)	h	hot side
h	enthalpy($J\ kg^{-1}$)	*i*	inner, *i*th grid
H	height (m)	is	isentropic
i, j, k	coordinates	*j*	*j*th grid
$\dot{m}$	mass flow rate ($kg\ s^{-1}$)	*k*	*k*th grid
P	pressure (Pa, bar)	min	minimum
$\dot{q}$	heat transfer per square meter ($W\ m^{-2}$)	max	maximum
$\dot{Q}$	heat transfer (W)	o	outer
R	resistance ($K\ W^{-1}$),ratio	p	pressure
s	perimeter of inner pipe (m)	r	refrigerant

TAT	transition airtemperature (°C)	wi	inner pipe wall
T,t	temperature (K, °C)	v	vapour, volumetric
u	velocity (m s^{-1})	l	liquid
UA	overall conductance (W K^{-1})		
Va	air face velocity (m s^{-1})		
W	width (m)		
z	length (m)		
α	heat transfer coefficient (W m^{-2} K^{-1})		
η	efficiency		
Δ	difference		
ρ	density (kg m^{-3})		
τ	shear stress (N m^{-2})		
ε	effectiveness		
$<\alpha>$	void fraction		
γ	compression index		

1. Introduction

As a natural refrigerant, carbon dioxide (CO_2) has been attracting increasing attention in the application areas of commercial refrigeration, heat pumps and air conditioning, as indicated by Nekså (2004). Compared to conventional refrigerants such as HCFCs (R22) or HFCs (R134a and R404A), CO_2 is more environmentally friendly due to its zero Ozone-Depletion Potential (ODP) and very low direct Global Warming Potential

(GWP<1), therefore attaining favourable thermophysical properties. These include higher density, latent heat, specific heat, thermal conductivity and volumetric cooling capacity, and lower viscosity. However, CO_2 has a relatively high operating pressure due to its low critical temperature (31.1 °C) and high critical pressure (73.8 bar).

Alongside all the other application areas, CO_2 has recently acquired significant attention for its application in supermarket refrigeration. The energy consumption of a typical supermarket in the UK is in the region of 1000 kWh/m^2 of which between 30% and 50% will be for refrigeration (Tassou (2007)). This large amount of energy consumption in the form of grid electricity contributes significantly to indirect CO_2 emissions and, consequently, global warming. Moreover, HFC refrigerants such as R404A, which is predominantly used in supermarket refrigeration systems, contribute extensively to direct CO_2 emissions. These direct emissions can reach up to 30% of indirect emissions, and thus the development and optimisation of systems employing the use of natural refrigerants, such as CO_2 is vitally important.

In general, two types of CO_2 refrigeration systems have been applied or are being considered for application in supermarkets: cascade systems (Eggen and Aflek (1998)) and all CO_2 transcritical systems (Nekså and Girotto (2002)). In a cascade system, CO_2 operating in a subcritical cycle is used in the lower cascade, with R404A, R134a, NH_3 or hydrocarbons such as propane employed in the higher cascade for heat rejection. In an all CO_2 system, if air cooling is used for heat rejection, which is predominantly the case, irrespective of the system arrangement employed, CO_2 will operate in a transcitical mode when the ambient temperature is high. The high pressure side heat exchanger in this system will act as either a gas cooler or a condenser, dependent upon the ambient temperature.

There are, conventionally, two refrigeration circuits in a supermarket refrigeration system arrangement: (i) medium temperature circuits for the chilled food display cabinets and chilled food cold rooms and (ii) low temperature circuits for the frozen food cabinets and frozen food cold rooms. These two temperature circuits can operate in parallel as in the cases with R404A systems and various CO_2 systems (Girotto et al. (2003)) or integrated, as shown with several all CO_2 systems (Schiesaro and Kruse (2002)). The cascade CO_2 system has numerous advantages, including greatly reduced low-temperature compressor sizes, the absence of a liquid pump, and fewer stages of heat transfer compared to compound or 'booster' systems (Kim et al. (2004)). It has also been reported that the energy consumption of the cascade system is neutral or less than that of conventional R404A systems (Christensen and Bertilsen (2003)).

For an all CO_2 system, reported advantages include simpler and cheaper system designs with one fluid and one circuit (medium temperature and low temperature) and a heat recovery potential. It has also been reported, however, that the total annual energy consumption of an all CO_2 system in a hot climate can be higher than that of a conventional R404A system (Girotto et al. (2004)). Systems installed in Northern European countries such as Sweden, Denmark, Germany and Switzerland, nonetheless, can attain an equivalent or lower annual energy consumption than R404A systems due to the higher number of hours during the year that such systems operate in the subcritical mode (Girotto et al. (2004)).

One method of improving the seasonal performance of an all CO_2 refrigeration system would be applying optimised control strategies for the system. Such control strategies can ensure that the system will operate efficiently in both transcritical and subcritical modes at all ambient temperature conditions. By means of mathematical

model, the optimised refrigerant discharge pressures were correlated to be increased lineally with higher ambient temperatures (Kauf (1999)). The correlation can be applied when the types and structures of system components are known such as heat exchangers and compressors. In addition, the low pressure side operating conditions such as pressure and superheat need also be specified. This method nevertheless does provide a useful guideline to predict the optimised discharge pressures at different operating conditions and various CO_2 transcritical systems. To maximise the total system COP (heating and cooling), the optimal refrigerant discharge pressures were correlated as a function of refrigerant temperatures at gas cooler outlet and evaporating (Sarkar et al.(2004)). The optimised pressures were increased with the higher gas cooler outlet temperatures but decreased with the enhanced evaporating temperatures. This correlation is also applicable for a particular system when the system component designs such as compressors are specified.

In this paper, a detailed procedure is described for the control of CO_2 cycles for medium temperature food retail refrigeration applications. The development of control procedures and strategies has been based upon a CO_2 system model. When the system operates in transcritical mode, the optimum refrigerant pressure and its variation with ambient air temperatures are predicted from thermodynamic cycle calculations. When the system operates in the subcritical mode, the conventional floating head pressure control strategy is employed wherein the condensing temperature (pressure) is controlled at a fixed value above the ambient temperature. The control strategy assumes a variable compressor speed and adjustable air flow for the gas cooler/condenser which can be modulated to meet the constant cooling load requirement at different ambient

conditions. Two ambient temperatures, 21 °C and 16 °C, are considered for transition between subcritical and transcritical operations.

2. Model description

The all CO_2 medium temperature supermarket refrigeration system is shown schematically in Figure 1, with its corresponding transcritical and subcritical cycles depicted in Figure 2. This system is composed of four main components: compressors, air-cooled condensers/gas coolers, expansion valves and display cabinet evaporators. The system model is an integration of a detailed condenser/gas cooler model with a simplified compressor model, an isenthalpic expansion process and constant evaporating temperature and superheating at the evaporator outlet. The detailed component models are described in the following sections.

2.1 Condenser and gas cooler model

The condenser or gas cooler is a type of finned-tube air-cooled heat exchanger and is modelled by the distributed method. This method is widely used in the modelling of condensers but rarely in the modelling of gas coolers (Ge and Cropper (2004)). Since CO_2 thermophysical properties change rapidly with temperature during an isobaric gas cooling process, it would be impractical to use the ε-NTU or LMTD method to simulate gas coolers (Kim et al. (2004)). The tube-in-tube method developed from the research of Domanski (1989) was employed in the simulation of a gas cooler by Chang and Kim

(2007). A gas cooler model was developed by Sarkar et al. (2006) by dividing the heat exchanger into several sections. The pressure drop calculations in both refrigerant and air sides were also reported. It is seen that the simulation accuracy can be further enhanced when the distributed modelling method is utilised. In this paper, considering the similarity, the combined model for condenser and gas cooler is described together using the distributed method.

To describe this modelling process, a diagram with the sub elements of the coil in a three-dimensional (3-D) space is shown schematically in Figure 3. In this diagram, tubes are arranged parallel to the *i* direction, *j* is specified in the longitudinal direction, while *k* is in the transverse direction. Air flows parallel to the *j* direction and refrigerant is assumed to flow in approximate counter-cross direction to the air flow. The selection of the number of small elements in the *i* direction is arbitrary, with a range from one to infinity. The larger this value, the more accurate the simulation will be, but expensive computing time will be required with diminishing accuracy. The coordinate value *i* represents the number of sub-elements for each pipe, *j* signifies the pipe number in the longitudinal path starting from air inlet to the heat exchanger, whilst *k* represents the tube number in the transverse path counting from the bottom of the heat exchanger.

With this arrangement, the state point of either the refrigerant or air at each specified sub-element in the 3-D space can be located with its corresponding coordinate values *i, j* and *k.* The modelling methodology is based upon the establishment of the conservation equations for each sub-element and an efficient routine to solve these equations. The solution and outputs from one sub-element are used as inputs to the next sub element with the simulation commencing from the refrigerant inlet. Initially, the corresponding

air side parameters are assumed and iterative calculations are completed until the calculated air parameters remain unchanged with any subsequent iteration.

2.1.1 Refrigerant side conservation equations

In the establishment of the refrigerant side conservation equations for each element, the following assumptions were made:

- System is in steady state
- No heat conduction within the longitudinal direction along the pipe axis
- Uniform heat exchanger air face velocity
- No contact heat resistance between fin and pipe
- The refrigerant at any point in the flow direction is in a thermal equilibrium condition

Mass equation:

$$\frac{d}{dz}[<\alpha>\rho_v u_v + (1-<\alpha>)\rho_l u_l] = 0 \quad (1)$$

Momentum equation:

$$\frac{d}{dz}[<\alpha>\rho_v u_v^2 + (1-<\alpha>)\rho_l u_l^2] = -\frac{dP}{dz} - \frac{\tau_{wi} s_{wi}}{A} \quad (2)$$

Energy equation:

$$\frac{d}{dz}[<\alpha>\rho_v u_v h_v + (1-<\alpha>)\rho_l u_l h_l] = -(\pi d_o / A_i)\dot{q} \quad (3)$$

It should be noted that the above three conservation equations are for the two-phase refrigerant region in the condenser. They are, however, also applicable for the single-phase regions of the condenser if the void fraction $<\alpha>$ is replaced by unity for the

vapour phase or zero for the liquid phase. For the gas cooler, the above conservation equations are applicable if the void fraction $<\alpha>$ is set to unity.

The conservation equations can also be used for the air side calculations. The pressure drop calculation is applied instead of the momentum equation and heat transfer calculation is included in the energy equation for this side. In addition, there is a heat balance between the air and refrigerant sides for each element.

2.1.2 Airside Heat Transfer

The ε- NTU method is used in the calculation of the air side heat transfer. For a single grid on the air side,

$$\dot{Q}_a = \varepsilon C_{\min}[T_r(i,j,k) - T_a(i,j,k)] \tag{4}$$

where, the effectiveness ε is calculated from:

$$\varepsilon = 1 - \exp(-\gamma \frac{C_{\max}}{C_{\min}}) \qquad \text{for } C_{\max} = C_h$$
$$\textit{where } \gamma = 1 - \exp(-\frac{UA}{C_{\max}}) \tag{5}$$

and,

$$\varepsilon = \frac{C_{\max}}{C_{\min}}(1 - \exp(-\gamma \frac{C_{\min}}{C_{\max}})) \qquad \textit{for } C_{min} = C_h$$
$$\textit{where } \gamma = 1 - \exp(-\frac{UA}{C_{\min}}) \tag{6}$$

The overall heat transfer coefficient can be calculated as:

$$UA = (\frac{1}{\alpha_a \eta_0 A_0} + \sum R_i + \frac{1}{\alpha_r A_r})^{-1} \tag{7}$$

where ΣR_i is the sum of heat conduction resistances through the pipe wall and collared fin.

The heat transfer from airside can be calculated as:

$$\begin{aligned}\dot{Q}_a &= \dot{m}_a(i,j,k)\times Cp_a(i,j,k)\times[T_a(i,j+1,k)-T_a(i,j,k)] \\ &= UA(i,j,k)\times[T_r(i,j,k)-T_a(i,j,k)]\end{aligned} \tag{8}$$

The parameters at grid points (*i+1, j, k*) for refrigerant and (*i, j+1 ,k*) air can be obtained when equations (1) to (3) are discretized and solved together with equations (4) to (8).

Accurate model predictions also rely upon the precise calculations of fluid properties, heat transfer coefficients and pressure drops on both refrigerant and air sides. The CO_2 refrigerant properties are calculated using subroutines from the National Institute of Standards and Technology software package REFPROP (McLinden et al. (1998)). The Dobson and Chato (1998) correlation is used for the calculation of the refrigerant heat transfer coefficient in the two-phase region of the condenser. For the single phases of the condenser, the calculation of the heat transfer coefficients for refrigerant flow in tubes is based upon the Dittus-Boelter correlation (Incoprera and DeWitt (1990)). The correlation from Müller-Steinhagen and Heck (1986) is used for the refrigerant two-phase friction pressure drop prediction in the condenser. The calculation of refrigerant heat transfer coefficient in the gas cooler uses the correlation by Pitla et al. (2002). The Blasius equation (Incropera and DeWitt(1996) is employed in the prediction of refrigerant pressure drop in the gas cooler. In addition, the air side heat transfer and friction coefficients are computed using the correlations by Wang et al (1999,2001).

2.2. Compressor model

An open-type compressor is assumed and modelled using the empirical correlations from Brown et al (2002) for volumetric and isentropic efficiencies.

The volumetric efficiency can be calculated from:

$$\eta_v = 0.8263\left[1 - 0.09604(R_P^{\frac{1}{\gamma}} - 1)\right] \quad (9)$$

and the isentropic efficiency from:

$$\eta_{is} = 0.9343 - 0.04478R_p \quad (10)$$

3. Model validations

The finned-tube air-cooled condenser model has been validated previously by comparing the model with test results (Ge and Cropper (2004)). Therefore, only the validation of the gas cooler model is described in this paper.

Detailed test results published by Hwang et al. (2005) were used for the validation, of which were obtained on a test facility developed for the evaluation of components for transcritical CO_2 systems. The test facility consisted of two environmental chambers which established the conditions for the evaporator and gas cooler/condenser respectively. Using this facility, numerous parametric tests were carried out on a CO_2 gas cooler. Varied parameters included inlet air temperature and velocity, refrigerant inlet temperature, mass flow rate and operating pressure.

A schematic diagram and flow arrangement of the gas cooler is shown in Figure 4 and specifications are listed in Table 1. To measure the variation of refrigerant temperature along the heat exchanger pipes, a number of thermocouples were attached to the outer surface of the pipes at the refrigerant inlet and outlet and to the U-bend

pipes. These thermocouples were well-insulated to guarantee accuracy in their temperature measurement.

Figures 5 and 6 display a comparison between simulation and test results for refrigerant temperature along the length of the gas cooler under different test conditions. It is noticeable from both the simulation and test results that most cooling occurs in the first few pipes, with the rapid reduction of refrigerant temperature and almost linearly up to pipe 6. The rate of cooling then reduces and plateaus at around pipe 27. Figures 5 and 6 also illustrate that for a constant refrigerant and air inlet temperature, the higher the air face velocity the higher the cooling rate of the refrigerant. This is evidently attributable to the impact of air velocity on the air side heat transfer coefficient.

The comparison between test and simulation results show that in the first few pipes the simulation under predicts the refrigerant temperature in the pipes particularly at the lower air face velocity of 1.0 m/s. This may be due to under prediction of the air side heat transfer coefficient at low velocities and high temperature differences such that this area requires further investigation. The impact of the simulation error in the first few pipes upon the overall simulation of the gas cooler, however, is fairly insignificant. The principal feature of the simulation employed in this paper is the simulation accuracy of the refrigerant outlet temperature of the gas cooler. Figure 7 compares the test and simulation results of the gas cooler refrigerant outlet temperature with error lines of $\pm 2.0\ ^{o}C$ and displays the vast majority of the results falling within the $\pm 2.0\ ^{o}C$ error lines.

4. Development of control strategies

To achieve an optimum performance, various control strategies are implemented dependent upon whether the system operates in the transcritical or subcritical mode. The mode of operation is determined by the Transition Air Temperature (TAT) which is a design parameter. This temperature primarily depends upon the effectiveness of the gas cooler and has been steadily increasing in the recent years due to the innovated designs of more effective gas coolers.

Thermodynamic analyses of the CO_2 system indicate that whilst the system operates in the transcritical mode, there is an optimum discharge (or 'head') pressure that maximises the system COP. The variation of this optimum pressure with the ambient air temperature is shown in Figure 8 for a gas cooler approach temperature of 3 K, a constant evaporating temperature of - 10 °C and 10 K superheat at the evaporator outlet. The approach temperature for a heat exchanger is defined as the as the minimum temperature difference between the two fluids. In this paper, for an air-cooled gas cooler, the approach temperature is assumed to be the temperature difference between refrigerant outlet and incoming air inlet. This shows that the optimum value of discharge pressure increases with higher ambient temperature of above 25 °C. For instance, at an ambient temperature of 28 °C, the optimum discharge pressure is 80 bar giving a cycle COP of approximately 2.3. At a higher ambient temperature, such as 35 °C, the optimum discharge pressure increases to 93 bar and the corresponding COP drops to 1.8.

The discharge pressure can be controlled by the high pressure valve (HP control valve, Figure 1). A programmed controller is needed to calculate the pressure setting point as a function of ambient temperature. The inputs of the controller are the discharge pressure and ambient temperature and the output from the controller will

modulate the high pressure valve. The variation in discharge pressure in response to changes in ambient temperature will instigate the approach temperature of the gas cooler to diverge away from its design value. A constant approach temperature can be maintained by modulating the coolant flow rate across the gas cooler through the use of variable speed fans. A variable frequency drive (VFD) system can be installed to modulate the frequency of the electrical power supplied to the fan motor in order to control the air face velocity. It is noted that the fan power consumption of condensers or gas coolers in a refrigeration system is normally about 5% or less of those consumed by compressors. Therefore somewhat air flow increase by modulating the fan speed will increase fan power consumption but it will not be significant enough to affect the cooling COP or EER.

For a subcritical cycle, the maximum condensing temperature can not be higher than approximately 31 °C, a value very close to the critical point. For a conventional HFC or HCFC system which employs floating head pressure controls, the temperature differences between the condensing refrigerant and ambient air can be assumed as 15 K (Faramarzi and Walker (2004)). If the equivalent temperature difference is applied for a CO_2 system, the transition air temperature can be taken as 16 °C (Girotto et al. (2004)). Recent improvements in the efficiency of condensers and gas coolers, nonetheless, allow a smaller refrigerant-air temperature difference, such as 10 K, to be used and a transition air temperature of around 21 °C is currently applied successfully throughout the UK.

To investigate the effect of transition air temperature on system performance, the two transition temperatures of 16 °C and 21 °C have been considered in this study. For control stability, a dead band of ±1 °C was used for the two set-points. For both the

transcritical and subcritical modes of operation, the assumption stated that the system would employ compressor variable speed control to correspond with the cooling capacity of the system to the load. For floating 'head' pressure control in a subcritical operation the minimum condensing temperature for the refrigeration system was assumed as 10 °C (Girotto et al. (2004)).

In the case of the transition temperature of 16±1.0 °C, at ambient temperature below 15 °C, the condensing temperature and pressure reduces with a decreased ambient temperature until the condensing temperature reaches the minimum of 10 °C, which occurs at an ambient temperature of 10 °C-15 °C = -5°C (assuming a temperature difference of 15 K between condensing and ambient temperatures). For ambient temperatures below -5°C, a constant pressure will be maintained at around 45 bar. On the other hand, any ambient temperatures above 17°C will stimulate the system to operate in the transcritical mode. The discharge pressure will be kept constant at 80 bar with increasing ambient temperatures of up to 29°C. Any values above this temperature will control the discharge pressure to the optimum value, which subsequently increases with ambient temperatures as shown in Figure 8.

For the transition temperature of 21±1.0°C, at ambient temperatures below 20°C, the condensing temperature and pressure will be reduced with decreasing ambient temperatures until the condensing temperature reaches the minimum of 10°C. This will occur at an ambient temperature of 10°C-10°C=0°C (assuming a temperature difference of 10 K between condensing and ambient temperatures). For ambient temperatures below 0°C the pressure will be kept constant at around 45 bar. On the other hand, ambient temperatures above 22°C will induce the system to operate in the transcritical mode. A constant discharge pressure will be maintained at 80 bar with increasing

ambient temperatures of up to 29°C. As shown in Figure 8, any values above this temperature will monitor the discharge pressure to the optimum value.

When the ambient temperature is within one of the transition temperature periods, (16±1°C or 21±1°C), the discharge pressure will be maintained as one in the previous operation mode (transcritical or subcritical).

The variation of the controlled refrigerant discharge pressure with ambient air temperatures for the two transition temperatures of 16°C and 21°C is shown in Figure 9. The variation can be expressed mathematically by the equations 11 and 12 respectively.

When TAT=16±1°C,

$$P_{dis}(bar) = \begin{cases} 44.97 & \text{when } t_{amb} < -5°C \\ 1.352t_{amb} + 51.1 & \text{when } -5°C \le t_{amb} \le 15°C \\ 72.05 & \text{when } 15°C < t_{amb} < 17°C \text{ and subcritical cycle is on} \\ 80 & \text{when } 15°C < t_{amb} < 17°C \text{ and transcritical cycle is on} \\ 80 & \text{when } 17°C \le t_{amb} \le 29°C \\ 2.558t_{amb} + 5.792 & \text{when } t_{amb} > 29°C \end{cases} \quad (11)$$

and when TAT=21±1°C,

$$P_{dis}(bar) = \begin{cases} 44.97 & \text{when } t_{amb} < 0°C \\ 1.352t_{amb} + 44.34 & \text{when } 0°C \le t_{amb} \le 20°C \\ 72.05 & \text{when } 20°C < t_{amb} < 22°C \text{ and subcritical cycle is on} \\ 80 & \text{when } 20°C < t_{amb} < 22°C \text{ and transcritical cycle is on} \\ 80 & \text{when } 22°C \le t_{amb} \le 29°C \\ 2.558t_{amb} + 5.792 & \text{when } t_{amb} > 29°C \end{cases} \quad (12)$$

To establish the effect of the control strategies outlined above on the system performance, these strategies were applied to the simulation of the CO_2 refrigeration system model. The condenser/gas cooler was assumed to have equal characteristics to

those shown in Figure 4. To correspond with the compressor capacity to the condenser/gas cooler, a displacement of 2.75 m^3/h was selected for the open-type compressor and a constant evaporating temperature of -10°C and 10K superheat at the evaporator outlet were assumed for the simulations. For the base case, in a transcritical operation the approach temperature on the gas cooler outlet was attained as 3K and in a subcritical operation the degree of subcooling was rendered 5K.

Figure 10 shows the variation of the system cooling capacity and compressor power consumption with ambient temperature for the two transition temperatures. The variation of the system COP is shown in Figure 11.

For 16°C TAT, when the ambient temperature is below -5°C, both the condensing temperature and the evaporating temperature will be controlled to constant values and hence the cooling capacity, power consumption of the compressor and cooling COP will remain constant. When the ambient temperature is between -5°C and 15°C, the discharge pressure will increase with the ambient temperature, as indicated in Figure 9. This will cause an augmentation in the compressor power consumption and a reduction in both the cooling capacity and the cooling COP. At ambient temperatures between 17°C and 29°C, the discharge pressure will be controlled to a constant value and thus the compressor power consumption will remain constant. Nonetheless, the system cooling capacity will decrease due to the increased refrigerant temperature at the gas cooler exit which will further lead to a decline in the system cooling effect and, consequently, a reduction in the cooling COP. When the ambient temperature is above 29 °C, the power consumption of the compressor will increase, whilst both the cooling capacity and COP will decrease corresponding to higher ambient temperatures. This is because the controlled discharge pressure increases together with the elevated ambient

temperature. In the transition temperature period of 16±1°C, the system performance would depend upon the system operation mode. If the operation mode is subcritical, the compressor power consumption, cooling capacity and COP would all be unchanged. Supposing in this period the system is in transcritical mode, the compressor power will remain unchanged, whilst the cooling capacity and COP will decrease with higher ambient air temperatures. Similar trends can be applied to the system of 21 °C TAT but with different magnitude levels. The power consumption is never higher nor the cooling COP lower for 21°C TAT than those for 16°C TAT at different ambient temperatures. The cooling capacity for 21°C TAT is always greater than that of 16°C TAT when ambient temperature is below 15°C or above 22°C. At ambient temperatures between 15°C and 22°C, the cooling capacity for 21°C TAT would be lower if a system with 16°C TAT is in the transcritical mode; otherwise, it will be a higher capacity.

In supermarket applications, should the internal temperature and relative humidity be controlled by the air conditioning system to constant values, the load on each installed display cabinet needs to remain equivalent to the designed value despite any changes in the outside ambient temperature. The capacity of the refrigeration system is designed to coincide with the total load at a designed ambient air temperature which should be sufficiently high in order to minimise the design risk without excessively over-sizing the system. For the exemplar CO_2 system considered in this study, an ambient design temperature of 40^oC was selected, giving the cooling capacity for the system of 4.7 kW. At ambient temperatures below 40^oC, the system will have excess capacity comparable to the constant load by modulating the compressor motor frequency. A variable frequency drive (VFD) system can also be installed to control the frequency of the

electrical power supplied to the compressor motor. The rotational speed of the motor is therefore controlled.

The variation of the motor frequency with ambient temperatures is shown in Figure 12. Correspondingly, the variations of normalized compressor power consumption, cooling capacity and COP are shown in Figure 13. For a 16^{o}C TAT, when the ambient temperature is between 40^{o}C and 17^{o}C, the system is in a transcritical mode and both the motor frequency and the normalised compressor power consumption decrease alongside the lower ambient temperature. When the ambient is between 15^{o}C and -5^{o}C, the system is in a subcritical mode and the motor frequency and the normalized power consumption are both reduced with the lower ambient temperature. When the ambient temperature is further reduced from -5^{o}C, the system is still in the subcritical mode and both the motor frequency and the normalized power consumption remain unchanged at minimum values. In the transition temperature period between 15^{o}C and 17^{o}C, the motor frequency and the normalized power consumption are all unaffected in the subcritical mode but increase with the ambient temperature in transcritical mode. Similar trends can be found for the system with a 21°C TAT. However, the compressor power consumptions for 21°C TAT are always lower than or equal to that of a system with a 16°C TAT. The required motor frequency for a 21°C TAT is never higher than that of system with 16°C TAT when the ambient temperature is below 15°C or above 22°C. When the ambient temperature is between 15°C and 22°C, the motor frequency for 16°C TAT is lower should it be in transcritical mode and higher in a subcritical mode. For both TATs, the normalised cooling capacity can always be maintained in unison.

It should be noted that the proposed control strategies are based upon the assumptions of the 3K approach temperature at the gas cooler exit and the 5K subcooling at the condenser outlet. However, both the approach temperature and the subcooling will be affected by different ambient temperatures, and there are set requirements for the application of controls in order to maintain these two temperature differences. The effects of ambient temperature at various heat exchanger face velocities on the approach temperature and the subcooling were predicted by the developed model and are shown in Figure 14 for the approach temperature and in Figures 15 and 16 for the subcoolings at different TATs. At a specific ambient temperature, the approach temperature decreases with an increased air face velocity, while the subcooling increases with a higher air face velocity. At different ambient temperatures, the air face velocities ensure the constant approach temperature and the predictions for the subcooling are shown in Figure 17.

In addition to the ambient temperature and air face velocity, the refrigerant parameters at the heat exchanger inlet such as temperature, pressure and mass flow rate will also strongly affect the approach temperature and the subcooling. To fully comprehend the variation of the controlled air face velocity with the ambient temperature at different TATs, as shown in Figure 17, the effect of ambient temperature upon these refrigerant parameters requires careful consideration. For a 16°C TAT, when the ambient temperature is below -5°C, the refrigerant parameters at the condenser inlet do not vary with the ambient temperature. Thus, to maintain a constant subcooling, the air velocity requires an augmentation with a higher ambient temperature. When the ambient temperature is increased from -5°C to 15 °C, the refrigerant inlet temperature, pressure and mass flow rate all increase. These higher refrigerant inlet temperatures and

mass flow rates have negative trends to the subcooling but a higher inlet pressure will boost the subcooling. The interactions amongst these three parameters will render the initial rise in the air face velocity and reduction with a higher ambient temperature. When the ambient temperature increases from 17°C to 29°C, the system is in a transcritical mode but at a constant refrigerant discharge pressure and inlet temperature whilst the refrigerant mass flow rate rises owing to a higher motor frequency, as shown in Figure 12. Consequently, there is a slight increase in the air face velocity with a higher ambient temperature. When the ambient temperature is increased from 29 °C, the air face velocity experiences an abrupt rise due to an increased refrigerant pressure. When ambient temperature is further increased, the approach temperature has a trend to decrease and, to a certain extent, the air face velocity also reduces. In the transition temperature period of 16±1°C, the air face velocity increases with higher ambient temperature, unless the minimum air face velocity is achieved whereby the air face velocity remains the same. Similar results can be applied to the system with different TATs. However, the controlled air face velocity for a 21°C TAT is always higher than or equal to that of system with a 16°C TAT.

The system simulation procedure can therefore be generalised. When ambient air temperature is know, the refrigerant gas cooler outlet temperature and optimal discharge pressure will be determined according to constant approach temperature and equation (11) or (12). The refrigerating effect is then solved when the evaporating temperature and superheating at evaporator outlet are specified. The required refrigerant mass flow rate is subsequently calculated when the cooling load is given. The compressor motor frequency is then updated to satisfy the required refrigerant mass flow rate. Afterwards, the condenser or gas cooler model is run and the fan speed (air velocity) is modulated to

guaranty that the calculated approach temperature and subcooling are close to the designed values. As a result, the compressor power consumption and cooling COP are predicted.

The control strategies outlined above can be used to predict the seasonal compressor power consumption of a CO_2 refrigeration system. In this paper, weather data for the city of Glasgow in the UK was chosen for simulation. The hourly variation of the ambient temperature over an entire year in Glasgow is shown in Figure 18. This diagram highlights that for the majority of time, the ambient temperature is below 20^oC. To investigate the effect of transition temperatures upon the annual compressor energy consumption, annual simulations were performed for the two transition temperatures. The conclusive results, shown in Figure 19, were normalised against the power consumption of the system at a 40^oC ambient temperature. These results demonstrate that lower transition temperatures lead to higher compressor power consumptions, compared with higher transition temperatures. The annual electrical energy savings for the 21°C TAT over the 16 C TAT is at 18%.

5. Conclusions

A procedure has been established by means of system models and the calculations of thermodynamic cycles to explore optimal control strategies for transcritical and subcritical CO_2 cycles of medium temperature food retail refrigeration systems. The system model is an integration of a detailed condenser /gas cooler model, simplified compressor model, isenthalpic expansion process, and constant evaporating temperature and superheating. Two transition ambient temperatures of 16°C and 21°C from

subcritical to transcritical operations were investigated. The variations of controlled refrigerant discharge pressures and cooling COP with ambient temperatures for these two transition temperatures were proposed and thus calculated. The control strategy employs variable speed compressor controls, and variable speed condenser fan controls. The compressor speed and capacity was modulated to correspond to the system capacity which varies with the ambient temperature to the load. During the subcritical operation, the condenser subcooling is controlled to a fixed value of 5 K by varying the air flowrate across the condenser. In the transcritical operation, the gas cooler air flow rate is varied to maintain a constant approach temperature of 3 K. When applying the control strategies into system performance simulations, the system performance with a higher transition temperature is continuously more advanced than that with a lower transition temperature, although there are requirements for a higher air face velocity. Furthermore, seasonal simulations for the city of Glasgow have shown that using the proposed control strategy will lead to energy savings of approximately 18% with a transition temperature of 21^{o}C compared to 16^{o}C. The proposed control strategies can be applied to both the existing and new CO_2 refrigeration systems when subscritical and transcritical operations are employed.

Acknowledgements

The authors wish to acknowledge the Food Technology Unit of DEFRA for their financial support for this project and the contribution of the industrial collaborators, Bond Retail Services Ltd, Apex Air Conditioning, Doug Marriott Associates and Bowman Power.

REFERENCES

Brown J. S., Yana-Motta S.F., Domanski P.A., 2002 . Comparitive analysis of an automotive air conditioning systems operating with CO_2 and R134a, International Journal of Refrigeration 25 ,19–32.

Chang Y.S., Kim M.S. , 2007. Modelling and performance simulation of a gas cooler for CO_2 heat pump system. V13,n3, HVAC&R Research, May, 445-456.

Christensen K.G., Bertilsen P. , 2003. Refrigeration systems in supermarket with propane and CO_2-energy consumption and economy, 21st IIR international congress of refrigeration, Washington, D.C., USA.

Dobson M.K., Chato J.C., 1998. Condensation in smooth horizontal tubes. J Heat Trans Trans ASME, 120:193–213.

Domanski P.A., 1989. EVSIM-An evaporator simulation model accounting for refrigerant and one-dimensional air, NISTIR-89-4133. Washington, DC:NIST.

Eggen G., Aflek K., 1998. Commercial refrigeration with ammonia and CO_2 as working fluids, Natural Working Fluids ’98, IIR-Gustav Lorentzen Conference on Natural Working Fluids, Oslo, Norway, IIR, June 2-5.

Faramarzi R.T., Walker D.H., 2004. Investigation of secondary loop supermarket refrigeration systems, PIER Consultant Report, March.

Ge Y., Cropper R. ,2004. Air-cooled condensers in retail systems using R22 and R404A refrigerants, Applied Energy 78 ,95–110.

Girotto S., Minetto S., Nekså P. , 2003. Commercial refrigeration system with CO_2 as refrigerant experimental results, 21st IIR international congress of refrigeration,

Schiesaro P., Kruse H. , 2002. Development of a two stage CO_2 supermarket system, IIF-IIR, New technologies in commercial refrigeration, Urbana, Illinois, USA.

Girotto S., Minetto S., Nekså P. ,2004. Commercial refrigeration system using CO_2 as the refrigerant, International Journal of Refrigeration 27 ,717-723.

Hwang Y., Jin D.H, Radermacher R., Hutchins J.W., 2005. Performance measurement of CO_2 heat exchangers, ASHRAE Trans., 306-316.

Incoprera F.P., De Witt D.P., 1990.Fundamentals of heat and mass transfer. New York: John Wiley.

Incropera F.P., DeWitt D.P. ,1996. Introduction to heat transfer. 3rd ed. New York:John Wiley &Sons.

Kauf F.,1999. Determination of the optimum high pressure for transcritical CO2-refrigeration cycles, Int. J. Therm. Sci. 38, 325-330.

Kim M.H., Pettersen J., Bullard C.W. , 2004. Fundamental process and system design issues in CO_2 vapor compression systems, Progress in Energy and Combustion Science 30, 119-174.

McLinden M., Klein S.A., Lemmon E.W., Peskin A.P. ,1998. NIST thermodynamic and transport properties of refrigerants and refrigerant mixtures- REFPROP, v6.0, NIST Standard Reference database 23.

Muller-Steinhagen H., Heck K., 1986. A simple friction pressure-drop correlation for two-phase flow in pipes. Chem Eng Process 20, 297–308.

Nekså P., 2004. CO_2 as refrigerant for systems in transcritical operation, AIRAH's 2004 natural refrigerants conference, Sydney, 28-32.

Nekså P., Girotto S. , 2002. CO_2 as refrigerant within commercial refrigeration, therotical considerations and experimental results, 5th IIR-Gustav Lorentzen Conference on Natural Working Fluids, September 17-20, Guangzhou, China.

Pitla S.S., Groll E.A., Ramadhyani S. , 2002. New correlation to predict the heat transfer coefficient during in-tube cooling of turbulent supercritical CO_2. International Journal of Refrigeration 25, 887-895

Sarkar J., Bhattacharyya S., Gopal R.M., 2004. Optimization of a transcritical CO2 heat pump cycle for simultaneous cooling and heating applications. International Journal of Refrigeration 27,830-838.

Sarkar J., Bhattacharyya S., Gopal R.M., 2004. Transcritical CO2 heat pump dryer:Part 1. mathematical model and simulation. Drying Technology 24(12),1583-1591.

Tassou S. A., 2007. Potential for Solar Energy in Food Manufacturing, Distribution and Retrail, Report to DEFRA, AC045, 25 pgs.

Wang C.C., Jang J.Y., Chiou N.F., 1999a. A heat transfer and friction correlation for wavy fin-and-tube heat exchangers, Int. J. of Heat Mass Transfer 42, 1919-1924.

Wang C.C., Lee W.S., Sheu W.J., 2001. A comparative study of compact enhanced fin-and-tube heat exchangers, Int. J. of Heat Mass Transfer 44, 3565-3573.

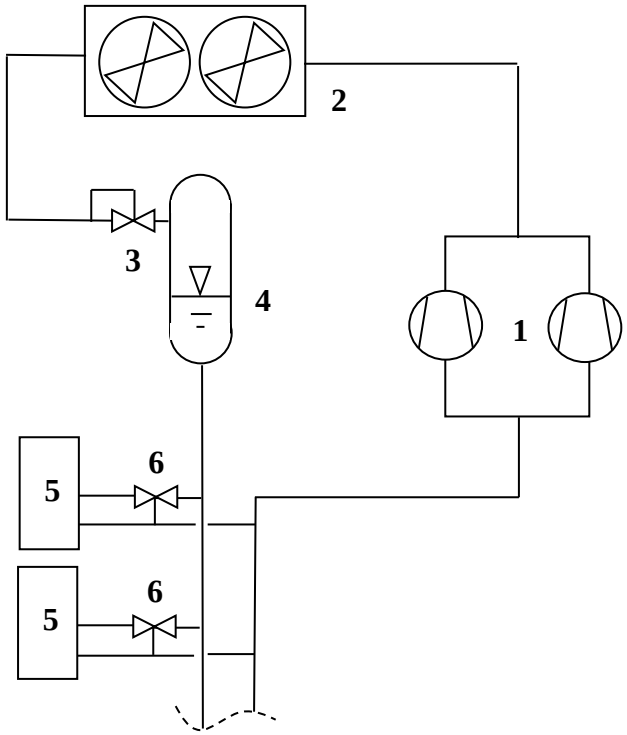

1-compressors; 2-condensers/gas coolers; 3-control valve;
4-liquid receiver; 5-display cabinets; 6-expansion valve

Fig. 1 - Schematic diagram of an all CO_2 medium temperature supermarket refrigeration system.

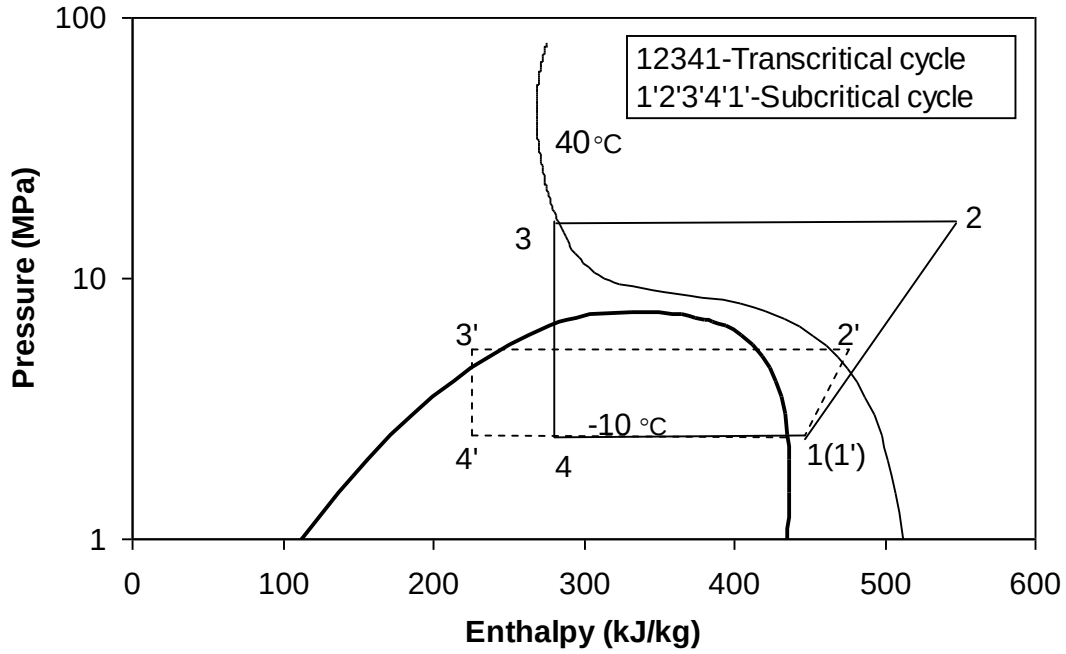

Fig. 2 - CO_2 transcritical and subcritical cycles with gas cooler outlet temperature of 40 °C and evaporating temperature of -10 °C.

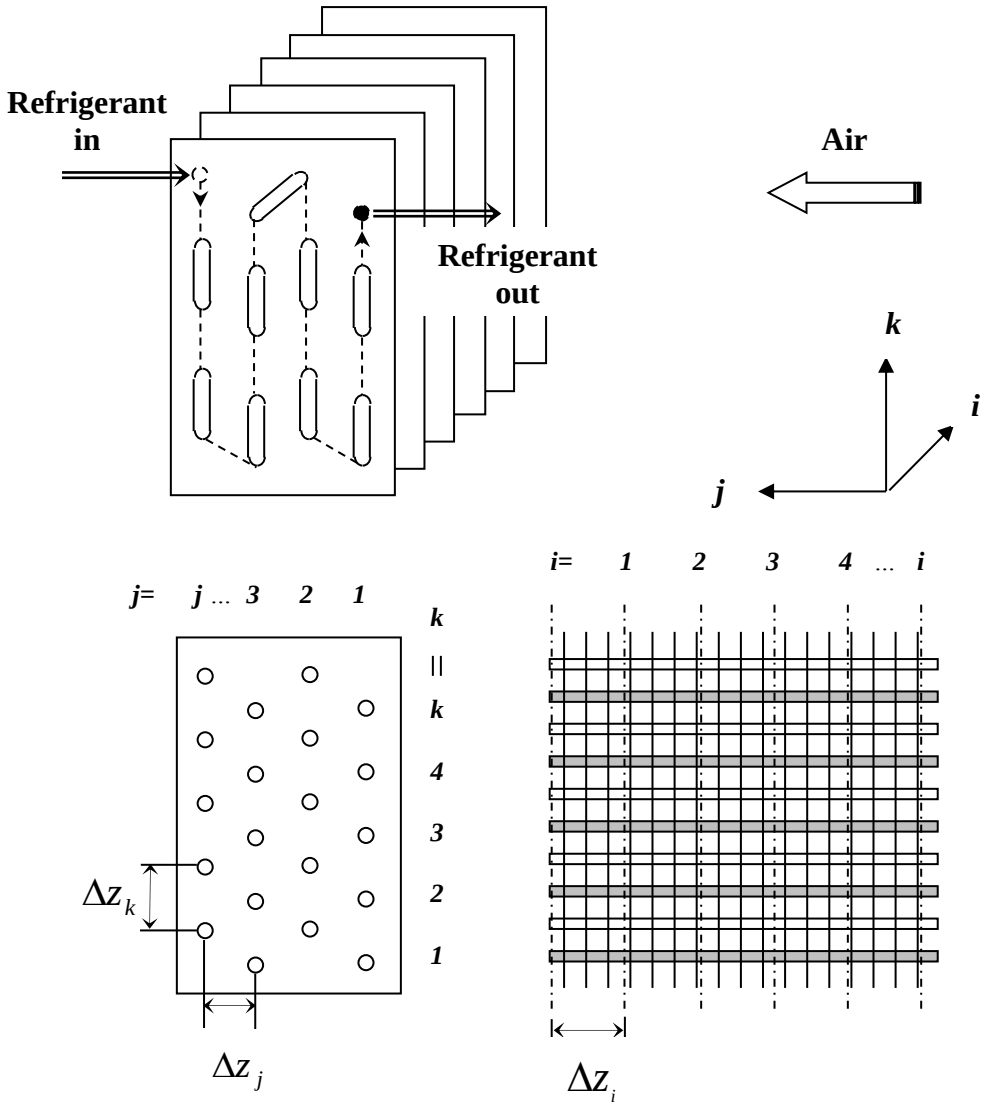

Fig. 3 - Three-dimensional coordinate of sub elements in the coil for the condenser/gas cooler model.

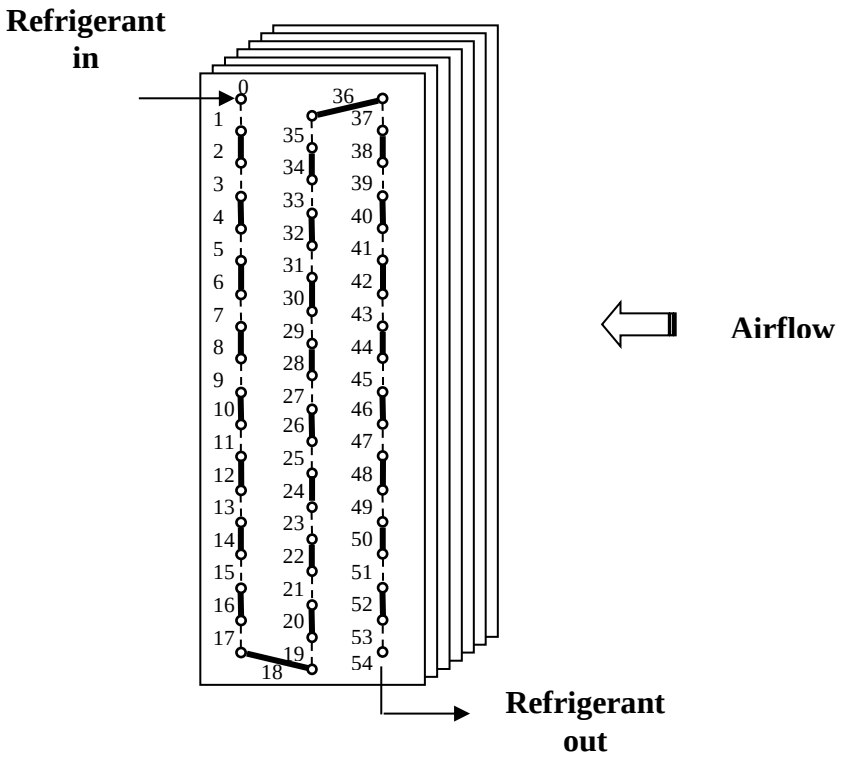

Fig. 4 - Tested gas cooler and numbered pipes.

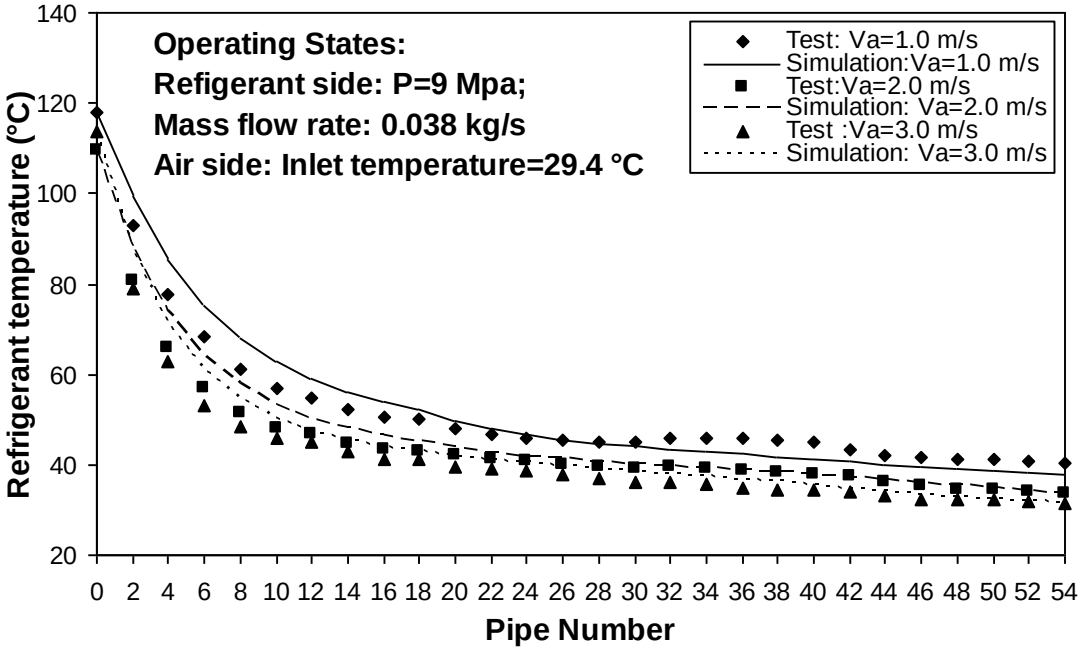

Fig. 5 - Comparison of simulation with test results for refrigerant temperature along the length of the gas cooler (1st set of test conditions).

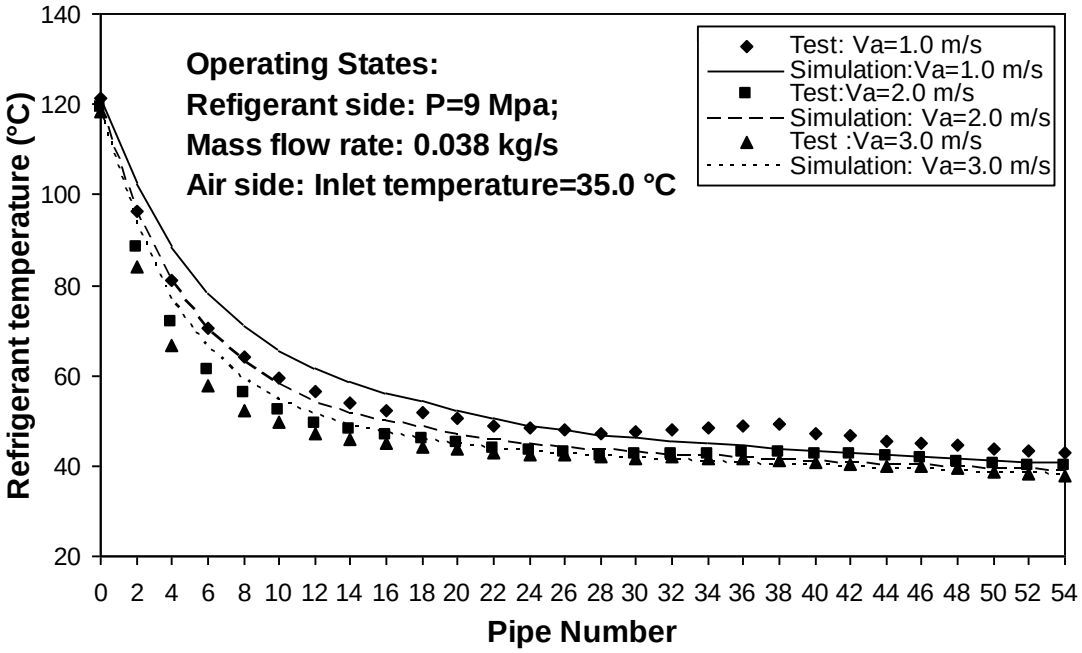

Fig. 6 - Comparison of simulation with test results for refrigerant temperature along the length of the gas cooler (2nd set of test results).

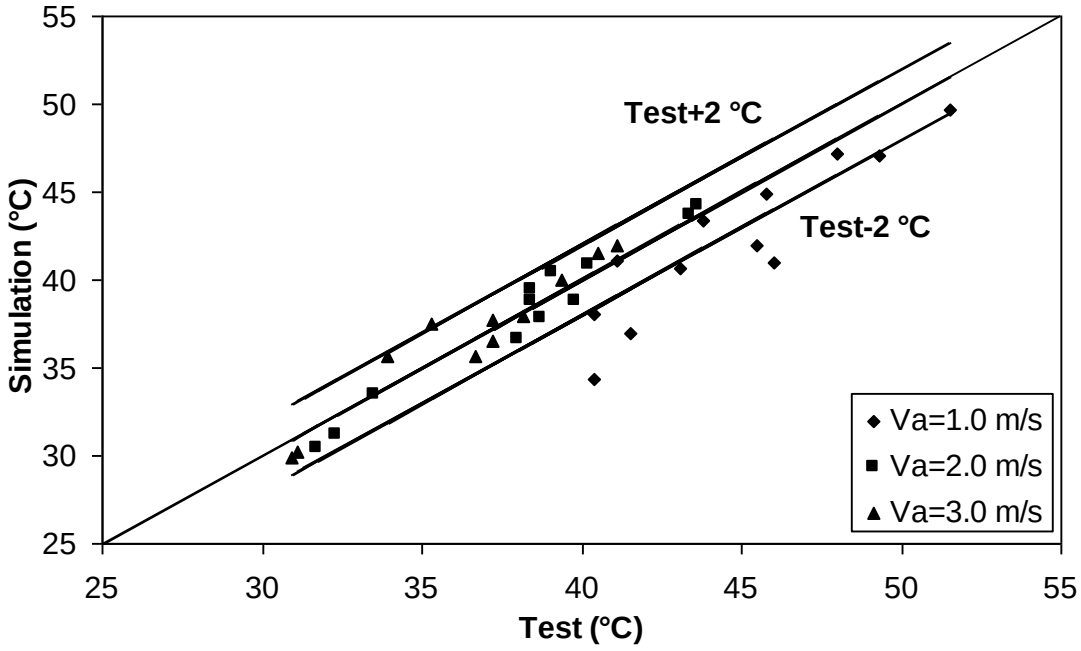

Fig. **7 - Comparison of simulation with test results for gas cooler refrigerant outlet temperature**.

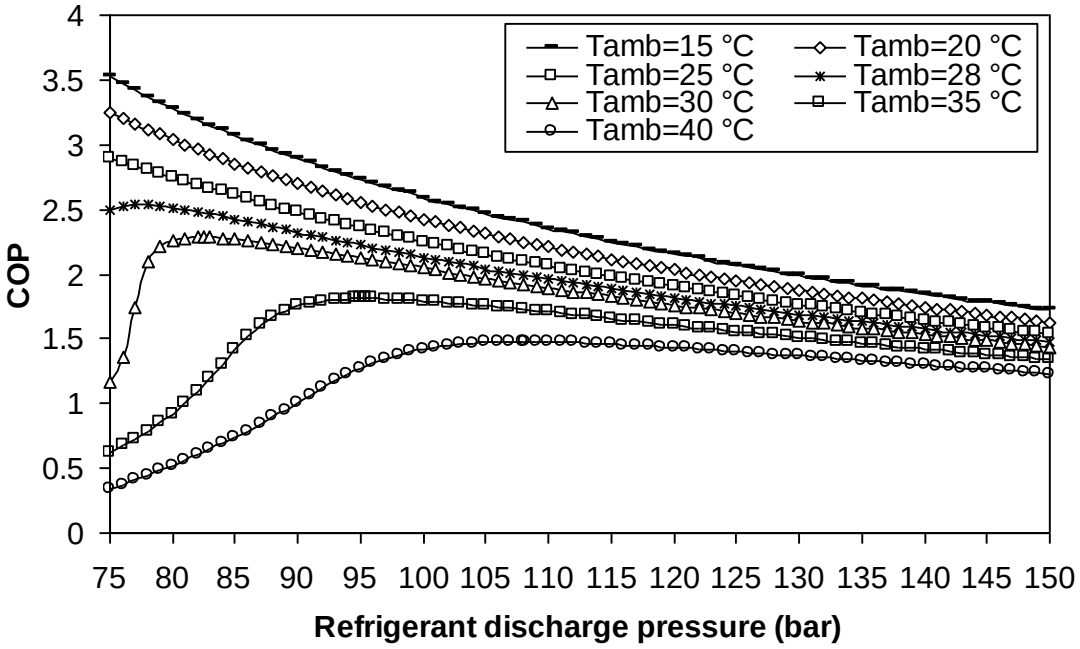

Fig.8 - Variation of cooling COP with refrigerant discharge pressure at different ambient air temperatures.

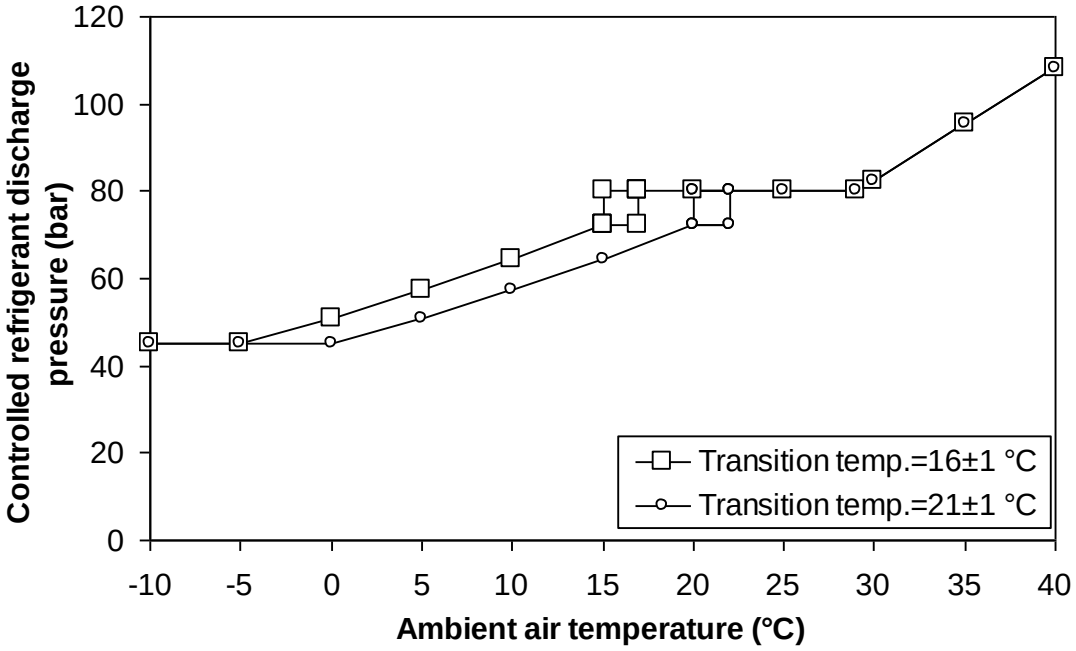

Fig. 9 - Variations of controlled refrigerant discharge pressures with ambient temperatures for the two transition temperatures.

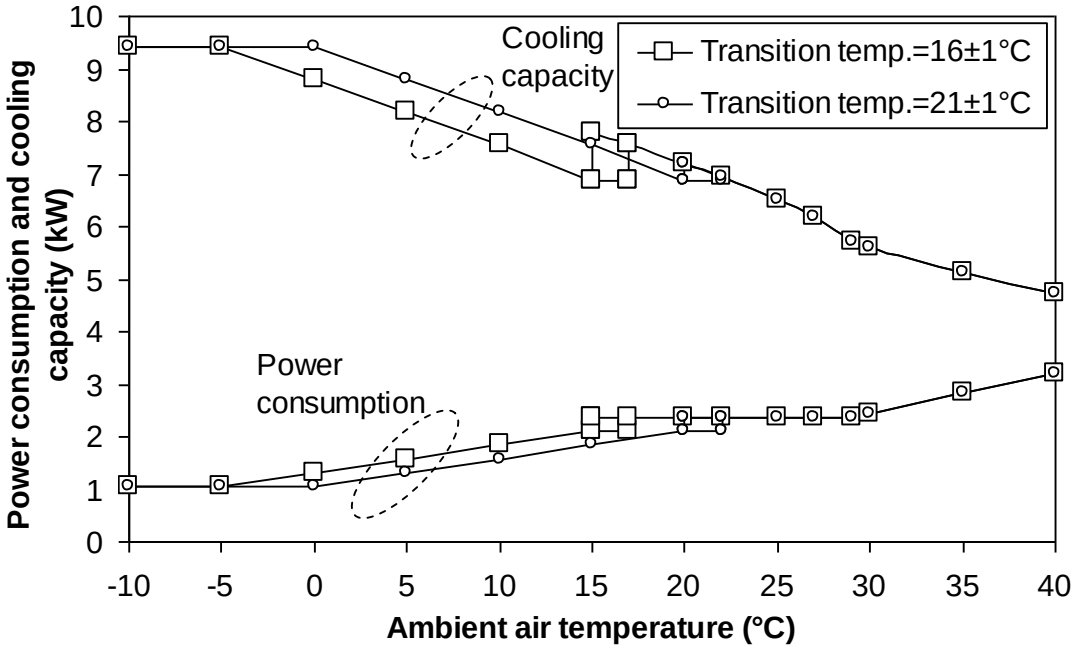

Fig. 10 - Variation of compressor power consumption and cooling capacity with ambient air temperature.

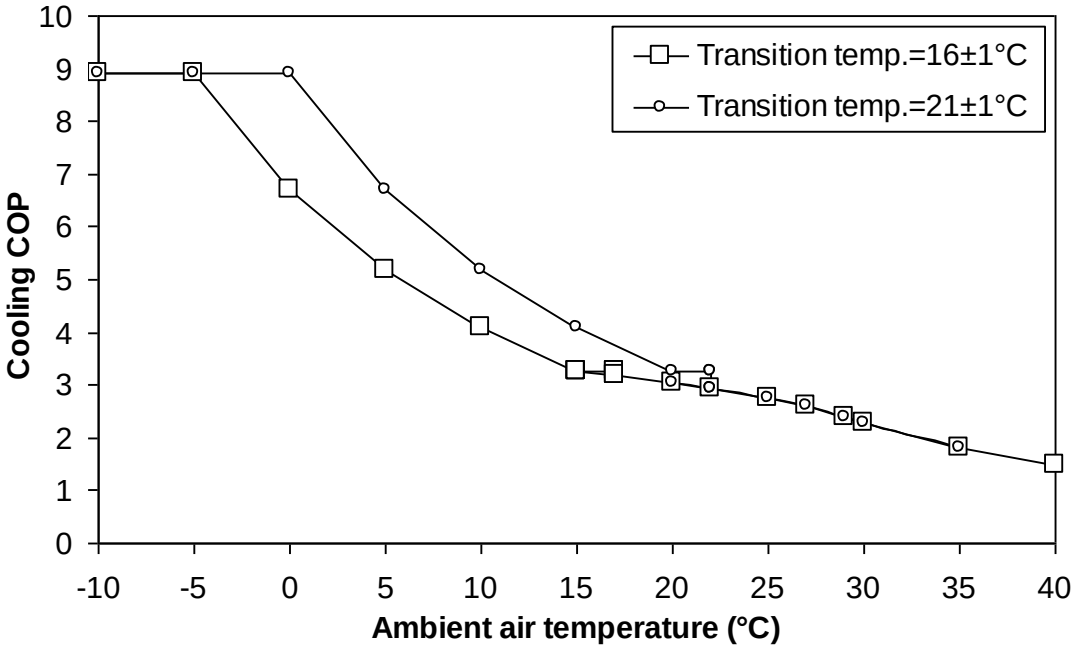

Fig. 11 - Variation of cooling COP with ambient air temperature.

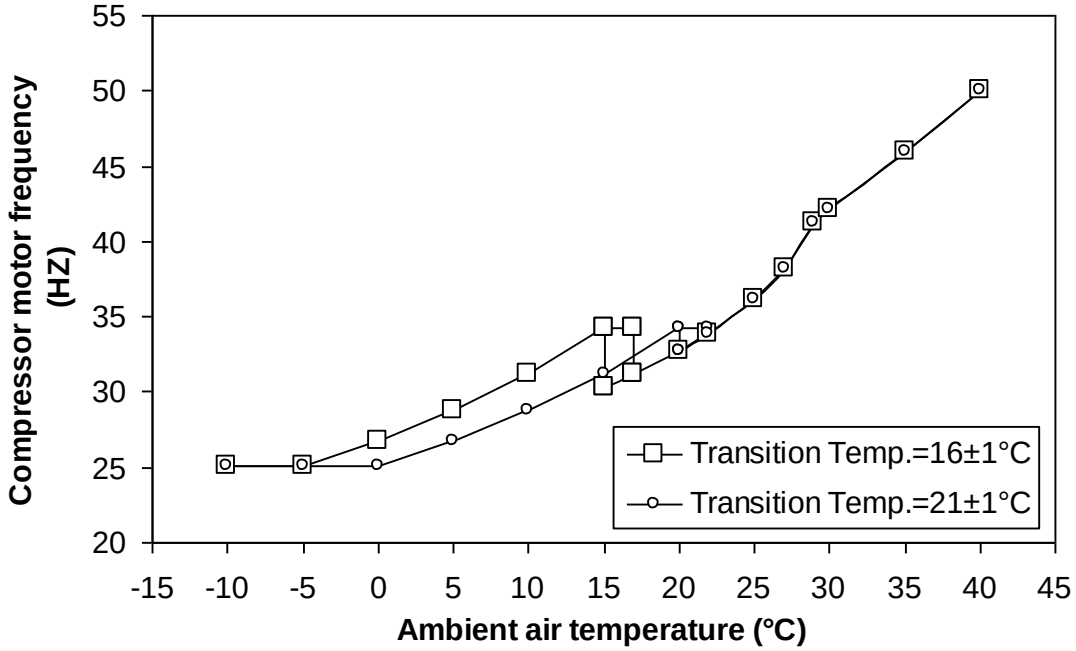

Fig. 12 - Variation of compressor motor frequency with ambient temperature.

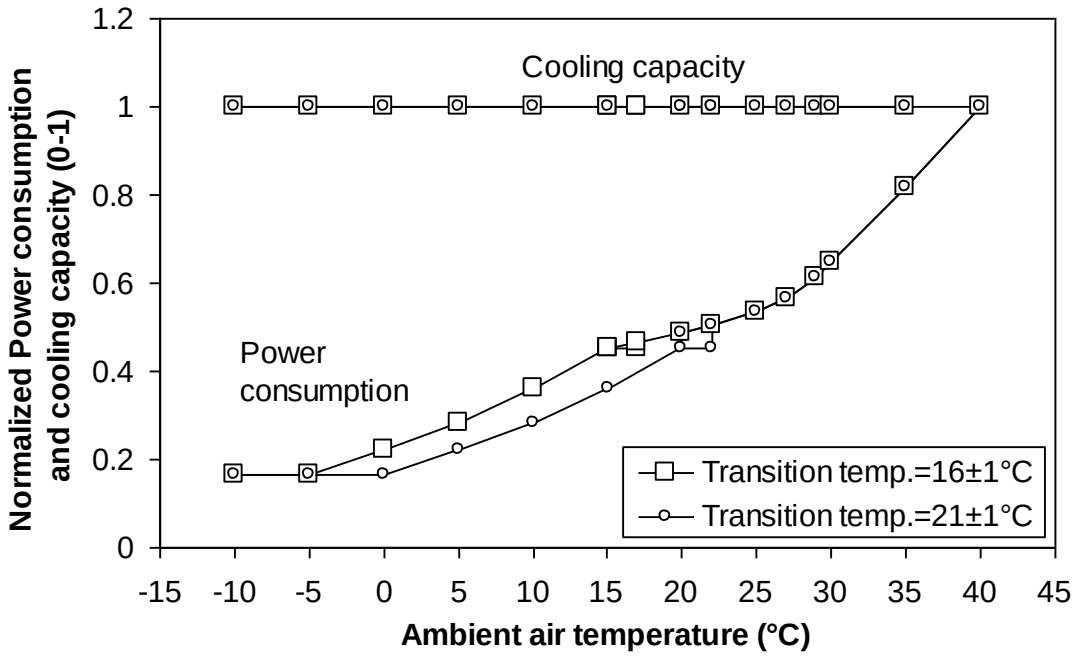

Fig. 13 - Variation of normalized power consumption and cooling capacity with ambient air temperature.

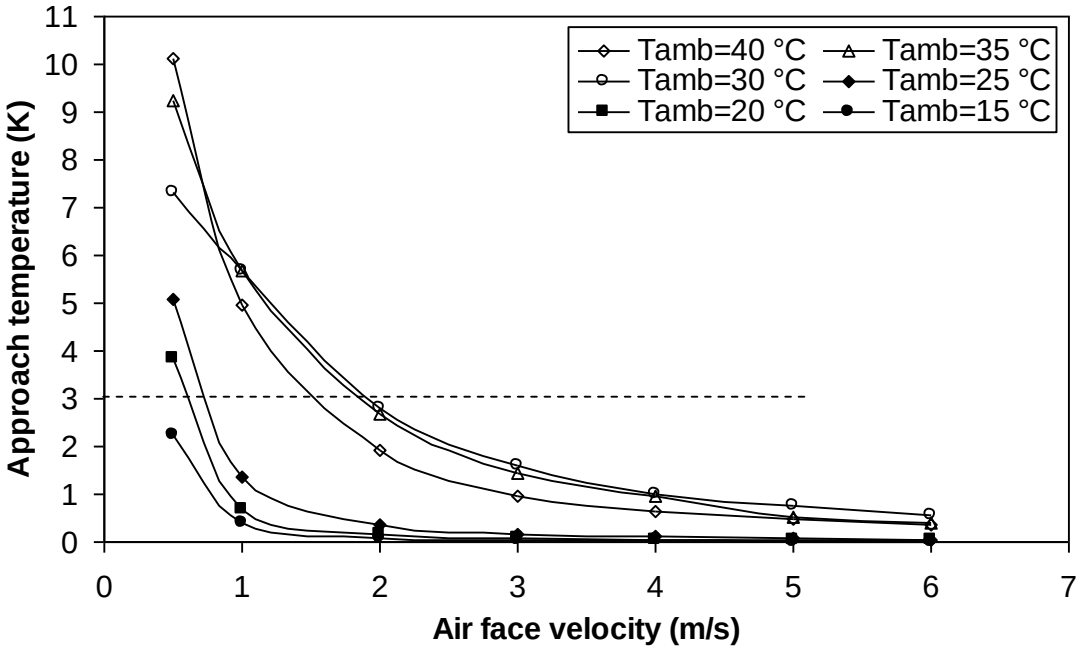

Fig. 14 - Variation of gas cooler approach temperature with ambient air temperature and face velocity.

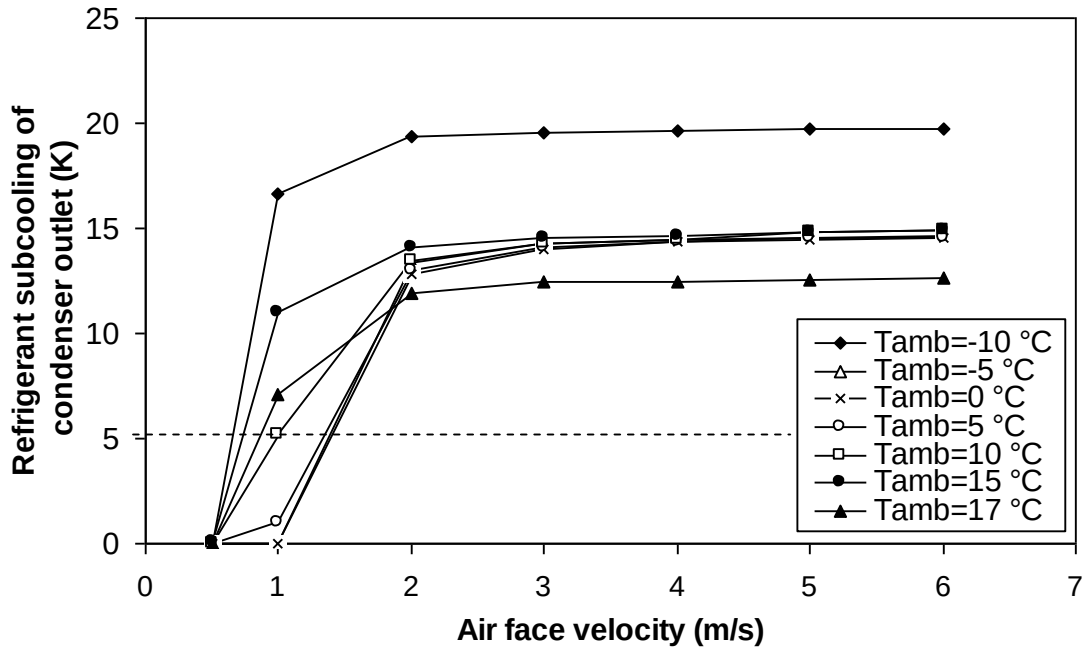

Fig. 15 - Variation of refrigerant subcooling at condenser outlet with ambient temperature and face velocity at 16 ^{o}C transition air temperature.

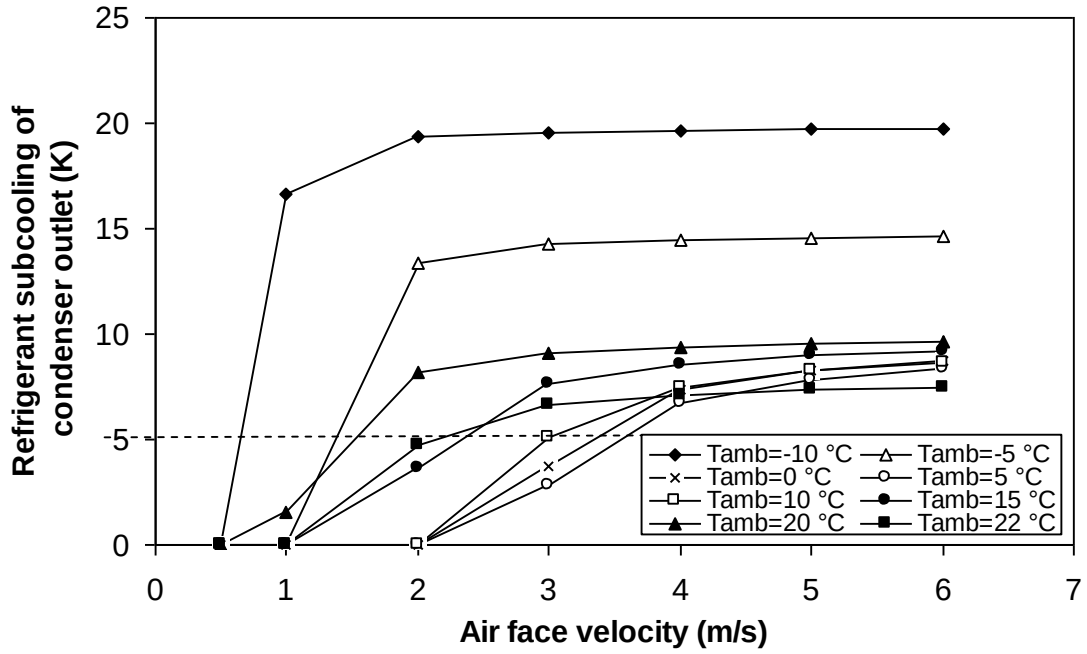

Fig. 16 - Variation of refrigerant liquid subcooling at condenser outlet with ambient temperature and air face velocity at 21 °C transition air temperature.

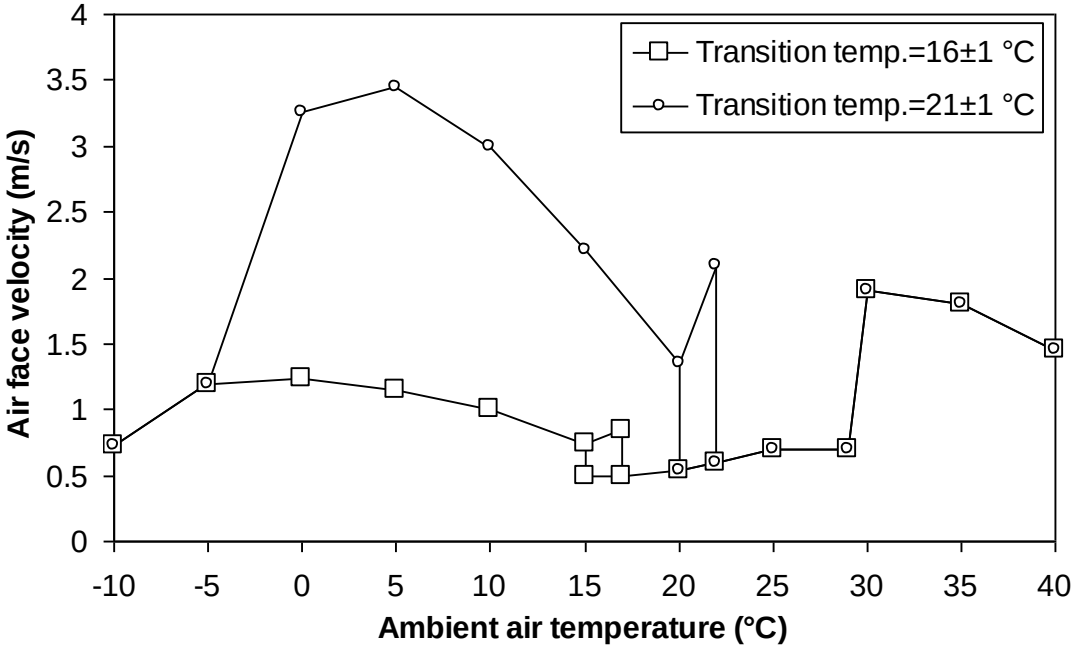

Fig. 17 - Variation of condenser/gas cooler air face velocity with AAT.

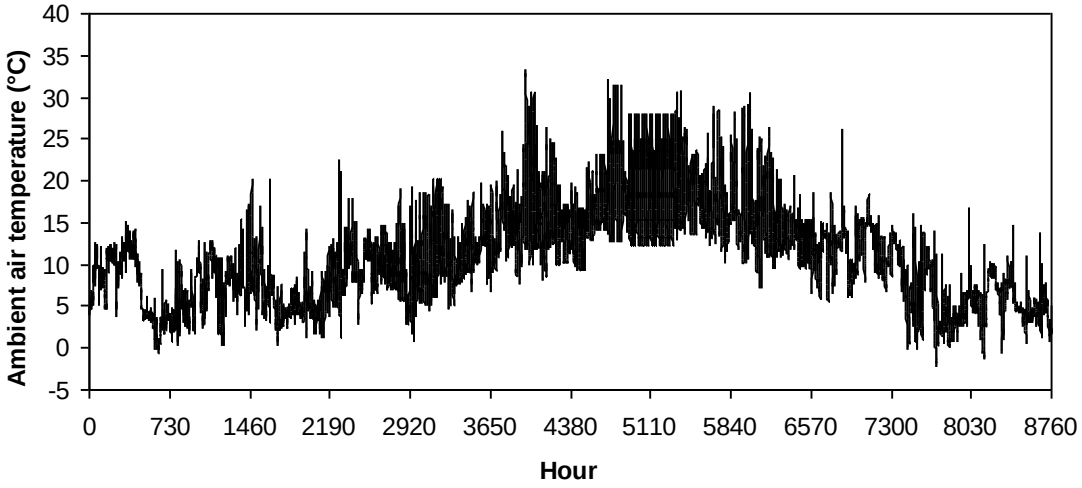

Fig. 18 - Hourly variation of ambient air temperature in Glasgow.

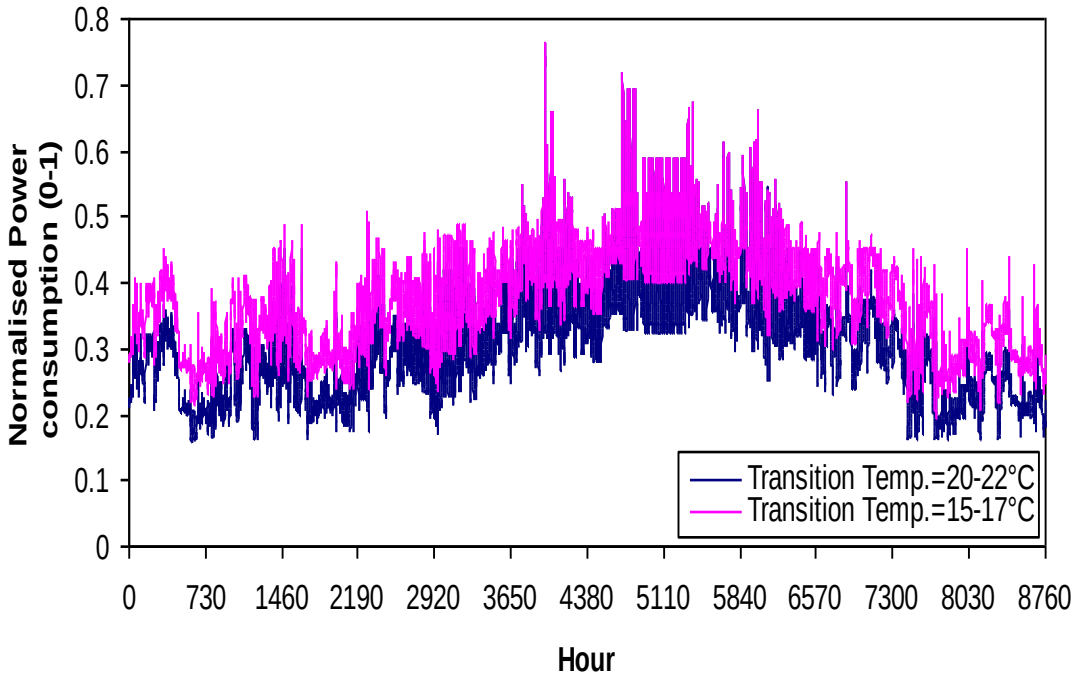

Fig. 19 - Hourly Variation of normalised compressor power consumption for the two transition temperatures over a year.

Table 1 Specification of the tested gas cooler

Parameters	Dimensions/Specifications
W×H×D (m)	0.61×0.46×0.05
Front area (m^2)	0.281
Shape	Raised lance
Fin pitch (mm)	1.5
Thickness (mm)	0.13
No. of tube rows	3
No. of tubes per row	18
Tube outside diameter (mm)	7.9
Tube inside diameter (mm)	7.5
Tube shape	Smooth